Conformational Space of 3-Chloropropionic Acid in Gas Phase Explored by Rotational Spectroscopy

Conformational space of 3-chloropropionic acid in gas phase explored by rotational spectroscopy

*Fufei Sun, Assimo Maris, Luca Evangelisti, Wentao Song and Sonia Melandri**

Department of Chemistry "Giacomo Ciamician", University of Bologna, Via Selmi 2, Bologna, Italy, sonia.melandri@unibo.it

J. Ricardo Morán, Camilla Calabrese, Alberto Lesarri*

Departamento de Química Física y Química Inorgánica, Facultad de Ciencias – I.U. CINQUIMA, Paseo de Belén, 7, 47011 Valladolid, Spain

KEYWORDS: Persistent and mobile organic chemicals, chloropropionic acid, conformational surface, structural determination, rotational spectroscopy, jet spectroscopy, nuclear quadrupole tensor

ABSTRACT

The conformational space of 3-chloropropionic acid has been studied in the isolated conditions of a supersonic expansion using Stark-modulated free-jet absorption millimeter-wave and centimeter-wave chirped-pulse Fourier transform microwave spectroscopy techniques. The rotational spectra originating from the three most stable conformers including ^{35}Cl and ^{37}Cl isotopologues were observed in both experiments using a helium expansion while a partial conformational relaxation involving skeletal rearrangements takes place in an argon expansion. The rotational parameters, geometries and energy order were determined from the experiment, allowing a comparison with quantum chemical predictions. B3LYP-D3(BJ)/Def2-TZVP performs slightly better than MP2/aug-cc-pVTZ in reproducing the molecular geometries. The deviations are higher for the conformers showing intramolecular interactions. It is also shown that the Douglas-Kroll-Hess second-order scalar relativistic core Hamiltonian approach in the point nuclear approximation is needed to accurately reproduce the electronic properties encoded in the fully determined nuclear quadrupole coupling constants tensors.

INTRODUCTION

Recently, Persistent and Mobile Organic Chemicals (PMOCs) have drawn attention because they can elude waste-water treatment facilities, subsurface environments, and even drinking water treatment processes.[1] The enrichment of PMOCs in the water cycle is attributed to their mobility which makes them challenging to remove in water treatment processes.[2] The two principal factors affecting PMOCs' mobility are water solubility and adsorption tendencies. These properties are both related to the molecule's polarity, which in turn is determined by the intrinsic structural properties and the influence of the intermolecular interactions including those with the solvent.

To model the mobility of PMOCs, approximate models based on the partition coefficient between octanol and water (K_{OW}) or the distribution coefficient (D_{OW}), which accounts for the concentrations of all forms of the compound (ionized plus uncharged), have been used.[3] However, it has been pointed out that for flexible molecules a proper modelling of the conformational ensemble is essential for the correct prediction of physical variables either in the isolated phase or in solution.[4]

The optimal experimental method for conformational studies is the use of a supersonic expansion coupled with high-resolution spectroscopic methods, which allow us to reveal the molecule inherent structural preferences.[5] In particular, pure rotational spectroscopy accurately identifies different tautomers, isomers or isotopologues by providing precise moments of inertia and structures both for molecules[6] or molecular complexes.[7] Moreover, observing an intense rotational spectrum requires a large permanent dipole moment, a characteristic of PMOCs, making them ideal candidates for such investigations.

The list of POMCs contains many halogenated compounds which are commonly used in various applications such as refrigerants, flame retardants, solvents, and pharmaceuticals.[8-13] Recently iodinated acetic acids and chlorinated propionic acids such as 3-chloropropionic acid (3ClPA) and 2-chloropropionic acid have been detected in drinking water during the screening of halogenated carboxylic acids.[13] In particular 3ClPA has broad applications in the chemical industry as an intermediate in the synthesis of various organic compounds and it plays a crucial role in the production of herbicides, insecticides, and other agricultural chemicals.[14] Since the substitution by a halogen atom can strongly affect the electronic properties and influence both intrinsic[15] and intermolecular behavior,[16, 17] understanding the conformational space of such compounds can be extremely valuable. For this reason, the focus of this work is the investigation of the potential energy surface (PES) of 3ClPA, with particular emphasis on the effects of halogen substitution on its molecular properties.

The non-substituted forms of carboxylic acids show two conformations of the acid group, illustrated in Figure 1 for formic acid. They are the *zusammen* (*Z*-COOH) and *entgegen* (*E*-COOH) forms but in the literature they are often referred to as *cis* and *trans* respectively so we will keep the double notation. For both formic and acetic acid, the *cis* (*Z*-COOH) conformation is the most stable. The relative energy difference between the *cis* and *trans* isomers of formic acid was determined by microwave relative intensity measurements to be 16.3(4) kJmol^{-1},[18] while for acetic acid it was calculated at 22.5 kJ mol^{-1}.[19] The *cis* (*Z*-COOH) conformation was the only one observed in gas phase[20-23] and Ar matrix[24] experiments on propionic acid. Two non-equivalent minima are present on the potential energy surface (PES, see Figure S1) of *cis* propionic acid. The *trans* (*E*-COOH) isomer was calculated to be at 20.7 kJ mol^{-1}.[24]

The gas phase studies on the halogen-substituted carboxylic acids indicate a great influence of the nature, number, and position of the substituted halogen atoms[25, 26] on the conformational space. Taking acetic acid as an example, we can see that substitution with a fluorine atom stabilizes the high-energy *E*-COOH, which becomes much closer to the *Z*-COOH form (2.5(1) kJ mol^{-1}).[25] Both conformations feature an antiperiplanar fluorine atom (F-C-C-OH dihedral angle ca. 180°) and the less stable form (*E*-COOH arrangement) takes on a cyclic arrangement with an stabilizing O-H···F intramolecular hydrogen bond.

In difluoroacetic acid, the presence of two fluorine atoms allows for a more complex PES (see Figure S2 for details on the PES of all fluorine derivatives). Indeed, two *Z*-COOH conformations have been observed by microwave spectroscopy where the methyl hydrogen atom is either *gauche* or *anti* with respect to the C-O bond (*E*(*gauche*)-*E*(*anti*)= 4.4±2.2 kJ mol^{-1}) based on relative intensity measurements.[27] Also, in trifluoroacetic acid the *Z*-COOH conformation, was observed in gas phase[28] while the higher energy *trans* (*E*-COOH) conformation was detected in different cryomatrices.[29] In the case of the mono-chloro[30] and mono-bromoacetic acid[26]a single *Z*-COOH conformation was observed, similar to fluoroacetic acid. Three conformations were suggested from the vibrational spectrum, but the this assignment is unclear (see Figure S3 for details on the PES of all chlorine derivatives).[31]

As regards the halogenated substituted species of propionic acid, only a small number of compounds have been studied by microwave spectroscopy, namely: 2-fluoropropionic acid[32] and 2-chloropropionic acid. [33] For 2-fluoropropionic acid[32] the *Z*- and *E*-COOH forms are almost isoenergetic and the *E*-COOH arrangement is the most stable one (energy difference 0.5±0.2 kJ mol^{-1}), while for 2-chloropropionic acid, only one *Z*-COOH conformation was observed, in which the chlorine atom is *gauche* with respect to the carboxyl group, and the terminal carbon atom is

anti with respect to hydroxylic group. Interestingly, another *Z*-COOH conformation was predicted to have an energy difference of 1.41 kJ mol^{-1} but was not observed in the jet expansion.[33]

In order to elucidate the still controversial conformational properties of propionic acids and understand the features attributable to the presence of chlorine we investigate in this work the conformational isomerism of 3ClPA in the gas phase by studying its rotational spectrum and comparing the results to quantum mechanical calculations. This comprehensive analysis has the potential to offer new insights into the properties of PMOCs.

METHODS

Experimental details

The rotational spectrum of 3ClPA was first measured using a Stark-modulated Free-Jet Absorption Millimeter-Wave (FJ-AMMW) spectrometer, which operates in the 59.6-78.3 GHz region and has been previously described.[34, 35] The 3ClPA sample (melting point 40 °C) was used without further purification and heated to 60 °C. An inert gas (argon or helium) was flowed over the heated sample container using a stagnation pressure of 18 kPa and 32 kPa respectively for argon or helium. The gas mixture was then expanded through a 0.3 mm diameter nozzle into a chamber to a final pressure of 0.2 Pa for the experiment with argon and 0.4 Pa for the experiment with helium. The estimated accuracy of the frequency measurements is about 50 kHz, allowing the resolution of lines separated by >300 kHz. An additional spectrum was obtained in the 2-8 GHz frequency range using a Chirped Pulse Fourier Transform Microwave (CP-FTMW) spectrometer. Here, helium was flowed over the sample of 3ClPA heated at 60°C. The backing pressure of helium was maintained at 203 kPa and the mixture expanded into the chamber, achieving a rotational temperature of about 2 K. The direct-digital CP-FTMW instruments uses an arbitrary-waveform

generator (25 MSamples/sec) digital source, followed by amplification with a travelling-wave tube (250 W). A set of eight chirp-pulses were used for each gas pulse. Transmission of the exciting radiation and signal reception used horn antennas, oriented perpendicularly to the jet. The estimated accuracy of the frequency measurements is about 10 kHz.

Computational details

A systematic survey of the PES of 3ClPA was conducted at the B3LYP-D3(BJ)/Def2-TZVP level of calculation. This method behaved satisfactorily in similar molecules.[36] Harmonic frequency calculations confirmed that the calculated structures correspond to real minima. The potential energy surface related to the CC-C(OH) and ClC-CC torsion angles for the *Z*-COOH conformation were obtained at the same level of calculation through relaxed scans using a 10° step in the full rotation cycle. The geometry of selected conformers was further optimized at the MP2/aug-cc-pVTZ level of calculations. The obtained structures were used to estimate the nuclear quadrupole coupling constants of the chlorine nucleus by using the Douglas-Kroll-Hess second-order scalar relativistic core Hamiltonian,[37] in the point nuclear approximation, with the recontracted aug-cc-pVTZ-DK basis set[38, 39] freely available at the Basis Set Exchange Database[40] (we indicate this method with the acronym MP2//DK). The computations used the Gaussian software package (G16, revision C.01).[41]

RESULTS AND DISCUSSION

Potential energy surface

The conformational space of 3ClPA is defined by two skeletal dihedral angles (τ_1=ClC-CC and τ_2=CC-C(OH)) and the dihedral angle describing the orientation of the carboxylic hydrogen atom (τ_3=HO-C=O, see Figure 2). Considering the possible values of τ_1 and τ_2, three orientations are possible: *Anti*, *Gauche*, and *Gauche*', while for τ_3 there are two planar arrangements: *E* and *Z*. We can therefore label the conformers using a three-letter code for the τ_1, τ_2, and τ_3 angles, for example, *AAZ* represents the rotamer with $\tau_1 \approx 180°$, $\tau_2 \approx 180°$, and $\tau_3 \approx 0°$. A second label in Roman numbers (I, II, III…) was added to characterize the energy order of the conformers. By systematic search of the conformational space, a total of seven non-equivalent species were identified. They are depicted in Figure 2, including the relative energy values (B3LYP-D3(BJ)/Def2-TZVP). The four *Z*-COOH species lie below 6 kJ mol^{-1}, while the three *E*-COOH species are much higher in energy (17 to 35 kJ mol^{-1}). The global minimum is the plane-symmetric (C_s) conformer *AAZ*-I, characterized by an all-*anti* molecular skeleton. The second (*G'AZ*-II) and third (*GGZ*-III) isomers both have the chlorine atom in the *gauche* orientation. The most stable *E*-species shows a weak interaction between the chlorine and the hydroxyl hydrogen atoms. The complete set of spectroscopic constants of the *Z*-species is given in Table 1, while the information on the *E*-species is listed in the Supporting Information (Table S1). All theoretical structures are reported in a public repository at this link: https://doi.org/10.6092/unibo/amsacta/7975. Except for the *AA* conformers, each species possesses an equivalent enantiomer with exactly the same energy and spectroscopic parameters. For example, the *GA* conformers are equivalent to the *G'A* ones where the chlorine atom is on the opposite side of the CCC plane. Other couples of equivalent arrangements are *G'A/GA, GG/ G'G'*, *AG/AG'* and *G'G/GG'*.

Concerning the relation between the transition intensities observed in the experimental spectra and the conformational population, it is known that the intensity of a transition line of the *i*-th conformer with number density N_i can be assumed to be proportional to $\mu_{gi}^2 N_i$, where μ_{gi} are the projections of the electric dipole moment of the *i*-th conformer along the principal inertial axes ($g = a, b, c$).

Before the expansion, the conformational populations correspond to those of the equilibrium Boltzmann distribution, taking also into account the number of equivalent conformations (degeneracy) and zero-point energy. Accordingly, the intensities of the transition lines of each conformer can be related to the relative populations in the jet by assuming that the molecular system has been brought close to thermodynamic equilibrium at the temperature after the adiabatic expansion of the inert gas. However, one must be aware that if the interconversion barrier between two conformers is low enough, relaxation processes may change the expected population ratio. In the reported experiments only conformations with a significant dipole moment and relative energies below 10 kJ mol^{-1} are expected to give rise to an observable spectrum.[42] Therefore, since the population of the most abundant *E*-species is predicted to be less than 0.5% of that of the global minimum, we focused on the four *Z*-species with total dipole moments between 1.9 and 2.9 D (Table 1).

Rotational spectrum and conformational population

The spectrum of 3ClPA was initially recorded using argon as the carrier gas and the rotational lines belonging to two conformers were successfully identified with the FJ-AMMW spectrometer. The nuclear spin (*I*) of 3/2 for both ^{35}Cl and ^{37}Cl isotopologues gives rise to a hyperfine structure in the rotational transitions due to the interaction of the chlorine nuclear quadrupole moment with

the electric field gradient at the chlorine nucleus. For this reason, most transitions exhibited small hyperfine splitting (about 0.5 MHz) in the 59.6-78.3 GHz frequency range while the splittings were larger in the lower frequency range.. One example of resolved nuclear hyperfine structure of $3_{1,2} \leftarrow 2_{1,1}$ transition of ^{35}Cl-I is shown in Figure 4. The fitting procedure for the frequency components was performed in accordance with Watson's *S*-reduced Hamiltonian, implemented in Pickett's SPFIT program.[43, 44] The rotational Hamiltonian is as follows:

$$H = H_R + H_{CD} + H_Q$$

where H_R represents the rigid rotor part of an asymmetric top Hamiltonian, H_{CD} is the corresponding first-order centrifugal distortion, and H_Q takes into account the nuclear quadrupole interaction.[45]

The agreement between experimental and theoretical rotational parameters identifies the detected spectra to the two lowest energy conformations, namely: *AAZ*-I and *G'AZ*-II. Surprisingly, although *GGZ*-III and *AGZ*-IV were predicted to be energetically accessible, they were not observed in the spectra. As it is known, the carrier gas plays a role in the cooling process: heavier carrier gases enhance conformer interconversion[46] as observed, for example, for 1,3-propanedithiol[47] and 1,2-butanediol.[42] For this reason, the interconversion barriers between the most stable rotamers have been calculated. From the data reported in Figure 3, the calculated interconversion barrier from *GGZ*-III to *GAZ*-II (same as *G'G'Z*-III to *G'AZ*-II) is predicted to be about 10 kJ mol^{-1} while the barrier from *AGZ*-IV to *AAZ*-I (same as *AG'Z*-IV to *AAZ*-I) is only about 0.5 kJ mol^{-1}. As a 'rule of thumb', barriers greater than ~12 kJ mol^{-1} among conformers appear sufficient to trap population during the supersonic expansion in argon, while barriers lower than approximately 5 kJ mol^{-1} appear small enough to allow collisional relaxation.[48, 49] Relaxation

to more stable conformations is thus a possible explanation for the absence of *GGZ*-III and *AGZ*-IV in the argon expansion.

A partial confirmation of this arose from the observation of conformer *GGZ*-III when using helium instead of argon as the carrier gas while conformer *AGZ*-IV remained undetectable. We argue that *AGZ*-IV relaxes even when using helium which is quite unusual. A conformational relaxation in helium expansion was reported for 1-phenyl-2,2,2-trifluoroethanol with an interconversion barrier of 2.7 kJ mol^{-1}.[50] This was possible because in that case only a rearrangement of the light OH group was involved while relaxation of *AGZ*-IV to the global minimum *AAZ*-I in our experiment involves a reorientation of the heavy atom skeleton. Relaxation of *AGZ*-IV in helium expansion must be thus made possible by its very low conversion energy barrier.

Overall, for 3ClPA in helium expansion, the spectra of *AAZ*-I, *G'AZ*-II and *GGZ*-III were assigned both with FJ-AMMW and CP-FTMW. Conformer *AAZ*-I, characterized by zero μ_c component and appreciable values of μ_a and μ_b, exhibits an intense spectrum where μ_a-R-type and μ_b-R-type lines were observed (J'_{max} = 12, K'_{max}= 4). Several μ_b-R-type, μ_b-Q-type and μ_a-R-type transition lines were observed (J'_{max} = 24, K'_{max}= 9) for *G'AZ*-II, as expected for the large predicted values of μ_a and μ_b and the very low μ_c value. The observation of lower quantum numbers for the more stable *AAZ*-I conformer is due to the larger value of the *A* rotational constant with respect to that of *G'AZ*-II. Conformer *GGZ*-III shows a weak spectrum, where only μ_b-R-type lines were observed (J'_{max} = 15, K'_{max}= 7), in agreement with the large values of μ_b and small values of μ_a and μ_c. As regards the spectra of the ^{37}Cl isotopologues (natural abundance of ca. 24%) *G'AZ*-II and *GGZ*-III were observed in both experiments, while *AAZ*-I could be observed

only by CP-FTMW because of the very low intensity of its transitions in the higher frequency region covered by the FJ-AMMW spectrometer. The full NQC tensor could be determined for all species except ^{37}Cl -III for which only the diagonal terms were obtained while the off-diagonal ones were fixed to the fitted ^{35}Cl -III values scaled by the corresponding nuclear quadrupole moment values.[51] All observed lines were included in global fits for each conformation and each isotopologue and the results are reported in Table 2, while all measured rotational transition lines are listed in the Supporting Information (Tables S2-S7).

It is worth mentioning that a K_a=9←8 *Q*-branch of *G'AZ*-II was observed in the FJ-AMMW spectra recorded using both helium and argon. This allows to make an estimate of the rotational temperature of the adiabatic expansion in the different conditions by comparison with spectra simulated at different temperatures in Figure 5. The relative intensity measurements match with a rotational temperature of 10 K in the argon expansion and 18 K in helium, consistent with the greater rotational cooling efficiency of argon.[42]

From the recorded spectra it is also significant to estimate the relative populations of the identified conformers of 3ClPA by measuring the relative intensities of the rotational transitions: μ_b-R-type lines were used to estimate the population in Ar expansion, while both μ_a-R-type and μ_b-R-type lines were used for estimation in He expansion. Taking into account the calculated electric dipole moment components, we obtained an estimated population ratio of N_I: N_{II} = 1 : 0.25 in argon (no detection of III) and N_I: N_{II}: N_{III}=1 : 0.4 : 0.05 in helium. These ratios show that the calculated energy order is correct but they are not consistent with those predicted using the theoretical data (see Table 1). The derived population of the global minimum is higher than expected while those of conformers II and III are lower in both carrier gases. This disagreement could be due to the fact that a partial relaxation of the two higher energy forms onto the global

minimum occurs in the jet expansion or to the low accuracy of the calculated relative energy values. The observation that the populations of the two higher energy conformers are lower in argon expansion with respect to helium indicates a possible partial relaxation of these forms onto the global minimum in the argon expansion, while the doubt remains as to the fact that the lower populations of II and III in helium are due to relaxation processes or a relative energy higher than the calculated one. It must be noted that relaxation involving the carboxyl group in light carrier gas was observed also for alanine. [52]

Molecular structure

A comparison of the data reported in Tables 1 and 2 allows the estimation of the accuracy of the theoretical methods in reproducing the molecular geometries. As regards the global minimum *AAZ*-I, both methods perform similarly with deviation of the calculated and experimental rotational constants below 1%. For the other two conformations, *G'AZ*-II and *GGZ*-III, B3LYP-D3(BJ)/Def2-TZVP seems more accurate (deviations below 2%) than MP2/aug-cc-pVTZ (deviations up to 3.5%) suggesting that the B3LYP-D3(BJ)/Def2-TZVP method could better reproduce the interactions occurring in the *gauche* conformers.

A deeper analysis based on the planar moments of inertia (M_{gg} where g= *a, b, c*) shows that the greatest deviations are found for the M_{aa} values for all conformers. Regarding conformer *AAZ*-I, the M_{cc} planar moment of inertia is well reproduced (experimental value slightly larger than calculated ones) and its low value is consistent with the 4 out of plane sp^3 hydrogen atoms.

Using Kraitchman's equations[53] applied to the rotational constants of the ^{35}Cl and ^{37}Cl species, the substitution coordinates of the chlorine atom in the principal inertial axes system of the parent species were determined. The coordinates are obtained as absolute values, but their sign

can be reconstructed by comparison with theoretical calculations. Errors in the determined coordinates are calculated from propagation of uncertainties in the measured rotational constants, and then the usually much larger Costain's error is added.[54] They are shown in Table 3 and compared to the theoretical equilibrium values. In agreement with what was discussed in the previous paragraph regarding the moment of inertia, the DFT method overestimates the distance of the chlorine atom from the center of mass for all conformers while the *ab initio* method tends to underestimate them.

Nuclear quadrupole coupling tensor

Important information on the electron distribution is encoded in the nuclear quadrupole coupling (NQC) tensor, which is related to the electric field gradient (EFG) tensor at the involved nucleus. For example, the changes in the NQC-tensors at the chlorine and bromine atoms which take place upon perfluorination of aryl halides are a direct measure of the extent of the σ hole at the tip of the halogen atom.[16] It has also been shown that hydrogen bonding with water decreases the electric field gradient on nitrogen atom in *N*,*N*-diethylhydroxylamine.[55]

As shown in Table 2, the off-diagonal terms of the NQC tensor in the principal inertial axis system of the molecule (I-PAS) have been determined and thus, through direct diagonalization, the NQCs in the electric field gradient principal axis system (EFG-PAS) can be obtained. Their values and associated errors were calculated using the QDIAG program written by Z. Kisiel, available on the PROSPE website[56] and are reported in Table 4 for the parent species of the three observed conformers of 3ClPA together with their associated theoretical values.

The diagonalization process provides also the angles of rotation of the EFG-PAS (x, y, z) with respect to the I-PAS (a, b, c). The values can be obtained both from the experimental and

calculated values of the NQCs, supplying accurate benchmarks for different calculation methods. As regards the accuracy of the calculations in reproducing the NQCs of the chlorine atom we can see that B3LYP/Def2-TZVP overestimates the values while MP2/aug-cc-pVTZ underestimates them with a similar deviation (about 6-7%). A better agreement can be found using the MP2//DK method which accounts for relativistic effects (deviations around 3%). The better performance of the latter method was already shown in the study on chlorine and bromine-substituted benzenes.[16]

It can also be assumed that one of the EFG axis is coincident with the C-Cl bond and thus one can calculate the angles between the I-PAS and the C-Cl bond itself. These results are also shown in Table 4 and, albeit not totally coincident, they indicate that the *z* axis of the EFG system coincides with the C-Cl bond. The χ_{zz} values for conformers I, II and III (-71.6(3), -71.3(8) and -71.9(1) MHz, respectively) are equal within the error and the values of the asymmetry parameter ($\eta=(\chi_{xx}-\chi_{yy})/\chi_{zz}$) are very close to 0, indicating an almost cylindrical distribution of the electron cloud around the Cl-C bond. The value of χ_{zz} of 3ClPA is about 1 MHz bigger than that obtained for *trans*-chloropropane[57] (-70.68(11) MHz).

CONCLUSIONS

The conformational landscape of 3ClPA was explored by a combination of the rotational spectra in a supersonic expansion and extensive quantum chemical calculations aimed at reproducing the stable structures and their properties. Three conformers were observed in the gas phase, including both the ^{35}Cl and ^{37}Cl isotopologues in each case. For all observed species the carboxyl group is stabilized by adopting the *cis Z*-COOH arrangement. The three observed conformers of 3ClPA include the global minimum (*AAZ*-I), with all-*anti* coplanar atoms in the

heavy-atom skeleton and two other Cl-*gauche* conformations, *G'AZ*-II and *GGZ*-III. These isomers differ in the *gauche* or *anti* orientation of the carboxyl group.

The population distribution derived from the observed transition intensities confirms that the calculated energy order of the conformers is correct although the global minimum appears to be more populated than expected probably due to a partial relaxation occurring in the expansion and involving the carboxyl group.

A careful analysis of the structural parameters obtained from the isotopologues spectroscopic parameters, measured in natural abundance, further confirmed the assignment and allowed a comparison between the different quantum chemical methods. Both B3LYP-D3(BJ)/Def2-TZVP and MP2/aug-cc-pVTZ methods are accurate in reproducing the rotational parameters for conformer *AAZ*-I (deviations less than 1%) but somehow inaccurate for the *gauche* conformers (deviations up to 3.5%) probably due to a difficulty in describing the intramolecular interactions present in the latter conformations.

The electronic properties of the chlorine atom encoded in the nuclear quadrupole coupling constants were determined by diagonalization of the NQC tensor allowing a direct comparison with other molecules and the calculations. Indeed, the EFG shows a cylindrical arrangement around the Cl nucleus and the NQC constants' module along the CCl bond are equal for all conformers (average value -71.6(2) MHz) but slightly larger than the one determined for *trans*-chloropropan (-70.68(11) MHz).[57] Also, the best agreement between theoretical and experimental parameters is obtained when relativistic effects are accounted for.

Overall, the experimental and calculated data on 3ClPA show that the molecule possesses a complex conformational space and a careful use of experimental and theoretical tools was required to disentangle all its molecular properties.

ASSOCIATED CONTENT:

The computational data supporting the findings of this study are openly available in the University of Bologna repository at: https://doi.org/10.6092/unibo/amsacta/7975

Supporting Information.

Tables of spectroscopic parameters for *E*-COOH conformers, experimental transition frequencies for different conformations and ^{37}Cl isotopologues of 3ClPA (pdf). Potential energy diagram of the carboxyl group torsion for acetic acid and propionic acid and their fluorine and chlorine derivatives.

AUTHOR INFORMATION

Corresponding Authors

Sonia Melandri - Dipartimento di Chimica "G. Ciamician", Università di Bologna, via F. Selmi 2, 40126, Bologna, Italy; https://orcid.org/0000-0002-0410-5833; Email: sonia.melandri@unibo.it

Camilla Calabrese - Departamento de Química Física y Química Inorganíca, Facultad de Ciencias, Universidad de Valladolid, Paseo de Belén, 7, 47011-Valladolid, Spain; https://orcid.org/0000-0003-4299-2098; Email: camilla.calabrese@uva.es

Author Contributions

The manuscript was written through the contributions of all authors. All authors have given approval to the final version of the manuscript.

ACKNOWLEDGMENTS

SM, LE, AM and WS thank the Italian Ministry of Research (PRIN national project, grant n. J43C21000050001) and the University of Bologna for financial support (RFO). JRM, CC and AL thank the Spanish Ministerio de Ciencia e Innovación and the European Regional Development Fund (MICINN–ERDF) for funding support through projects PID2020-117925GA-I00, PID2021-125015NB-I00 and PID2022-136525NA-I00. The Junta de Castilla y León is thanked for funding project INFRARED IR2021-UVa13. FS acknowledges the China Scholarship Council (CSC) and the Marco Polo grant for financial support. JRM thanks the University of Valladolid for a predoctoral contract.

The authors thank the CINECA award under the ISCRA initiative, for the availability of high-performance computing resources and support.

Table 1. Predicted spectroscopic parameters for the four lowest-energy conformers of 3ClPA (B3LYP-D3(BJ)/Def2-TZVP and MP2/aug-cc-pVTZ).

	Conformers							
	AAZ-I		*GAZ/G'AZ* -II		*GGZ/G'G'Z*-III		*AGZ/AG'Z-IV*	
Parameters[a]	B3LYP	MP2	B3LYP	MP2	B3LYP	MP2	B3LYP	MP2
ΔE_e/kJ mol^{-1}	0.00	0.00	0.78	0.31	3.50	2.37	5.07	4.78
ΔE_0/kJ mol^{-1}	0.00	0.00	1.33	0.95	4.15	3.10	5.48	5.16
ΔG /kJ mol^{-1}	0.00	0.00	1.71	1.16	4.85	3.93	4.02	3.59
N_i/N_0 (333K)	1.0	1.0	1.24	1.42	0.45	0.65	0.28	0.31
N'_i/N'_0 (333K)	1.0	1.0	1.08	1.30	0.34	0.48	0.46	0.54
A / MHz	9267.01	9209.24	5498.09	5401.53	5066.85	4973.36	8870.06	8787.89
B / MHz	1167.95	1183.97	1548.80	1610.08	1648.97	1724.42	1177.60	1195.91
C / MHz	1050.62	1062.84	1523.16	1578.14	1613.67	1670.30	1078.40	1096.25
D_J / kHz	0.06	0.06	1.35	1.61	1.35	1.46	0.11	0.12
D_{JK} / kHz	0.83	0.88	-6.13	-6.90	-0.31	-0.43	5.95	7.58
D_K / kHz	7.56	7.40	36.28	38.51	10.20	7.97	20.48	24.49
d_1 / Hz	-0.01	-0.01	0.11	0.14	-0.20	-0.23	0.01	0.02
d_2 / Hz	-0.00	-0.00	-0.02	-0.01	0.01	-0.01	-0.00	-0.00
$3/2\chi_{aa}$ / MHz	-87.02	-76.50	11.55	15.01	17.02	19.01	-93.64	-82.81
$1/4\ (\chi_{bb}-\chi_{cc})$ /MHz	-4.73	-4.27	-0.86	-3.88	-21.94	-19.50	-0.43	-0.04
χ_{aa} / MHz	-58.01	-51.00	7.70	10.01	11.35	12.67	-62.43	-55.20
χ_{bb} / MHz	19.55	16.97	-5.58	-12.78	-49.56	-45.33	30.35	27.52
χ_{cc} / MHz	38.46	34.03	-2.12	2.77	38.21	32.66	32.08	27.68
χ_{ab} / MHz	-41.84	-37.35	36.80	-33.30	47.77	40.03	-28.43	-24.15
χ_{ac} / MHz	0.00	0.00	33.96	-26.12	4.12	6.14	25.00	23.36
χ_{bc} / MHz	0.00	0.00	-42.68	-38.65	-6.68	-11.40	7.56	0.12
$\lvert\mu_a\rvert$/D	1.64	1.58	1.24	1.11	-0.12	-0.12	0.100	0.76
$\lvert\mu_b\rvert$/D	0.93	0.83	2.25	2.21	2.69	2.72	1.68	1.57
$\lvert\mu_c\rvert$/D	0.00	0.00	0.06	0.13	0.77	-0.48	0.00	0.01
μ_{tot}/D	1.89	1.79	2.58	2.47	2.80	2.75	1.86	1.74
M_{aa}/uÅ^2	429.60	423.74	283.09	270.28	259.96	247.01	420.41	413.04
M_{bb}/uÅ^2	51.43	51.76	48.71	49.96	53.22	55.56	48.23	47.96
M_{cc}/uÅ^2	3.11	3.11	43.21	43.60	46.52	46.06	8.75	9.55
κ	-0.971	-0.970	-0.987	-0.983	-0.980	-0.967	-0.976	-0.974

[a] ΔE_e is the relative electronic energy. ΔE_0 is the relative zero-point corrected energy. ΔG is the relative thermal corrected Gibbs free energy (298 K; 1 atm)., N_i/N_0 is the population ratio of each conformer with respect to the global minimum calculated using the the relative zero-point corrected energy; N'_i/N'_0 is the population ratio of each conformer with respect to the global minimum calculated using the relative thermal corrected Gibbs free energies; A, B, and C are the rotational constants. D_J, D_{JK}, D_K, d_1, and d_2 are the quartic centrifugal distortion constants in the S-reduced semirigid rotor Hamiltonian. χ_{aa}, χ_{bb}, and χ_{cc} are the nuclear quadrupole coupling constants in the principal inertial axis system representation. μ_a, μ_b, μ_c are the electric dipole moment components. M_{gg} (g = a, b or c) are the planar moments of inertia, *i.e.* $M_{cc} = (I_{aa}+I_{bb}-I_{cc})/2$. $\kappa = (2B-A-C)/(A-C)$. κ is Ray's asymmetry parameter.

Table 2. The experimental parameters of the observed conformers of 3-chloropropionic acids.

Parameter [a]	^{35}Cl-I	^{37}Cl-I	^{35}Cl-II	^{37}Cl-II	^{35}Cl-III	^{37}Cl-III
A / MHz	9223.2548(41) [b]	9220.83(99)	5593.9084(12)	5563.4974(26)	5036.1680(30)	5008.8671(34)
B / MHz	1177.42396(39)	1145.88724(98)	1572.44126(41)	1537.34376(98)	1683.38610(81)	1647.8497(23)
C / MHz	1058.35711(35)	1032.72741(85)	1525.11070(38)	1492.1606(11)	1642.9555(13)	1606.3956(30)
D_J / kHz	0.0608(61)	[0.0608] [c]	1.33669(64)	1.306(12)	1.3983(78)	1.306(11)
D_{JK} / kHz	0.779(62)	[0.779]	-6.8684(82)	-7.008(69)	-0.292(53)	[-0.292]
D_K / kHz	6.96(17)	[6.96]	38.474(24)	38.553(78)	9.577(70)	9.703(51)
d_1 / kHz	-	-	0.12155(45)	0.105(27)	-	-
d_2 / kHz	-	-	-0.03269(29)	-0.0277(64)	-	-
$3/2\chi_{aa}$ / MHz	-81.301(13)	-64.222(15)	12.615(11)	9.093(13)	18.812(21)	14.073(65)
$1/4(\chi_{bb}-\chi_{cc})$ / MHz	-4.4624(46)	-3.4947(54)	1.8805(40)	0.6672(54)	-21.1595(73)	-16.592(13)
χ_{ab} / MHz	-39.49(44)	31.89(89)	32.75(82)	28.54(77)	42.54(26)	33.53*[d]
χ_{ac} / MHz	0	0	32.01(84)	24.52(86)	10.43(97)	8.22*
χ_{bc} / MHz	0	0	-40.718(37)	-31.963(45)	-7.02(16)	-5.53*
N	113	43	123	67	56	20
σ / kHz	23	6	19	15	25	25
μ_a / D	Y	Y	Y	Y	N	N
μ_b / D	Y	N	Y	Y	Y	Y
μ_c / D	N	N	N	N	N	N
M_{aa} / uÅ^2	425.9716(1)	437.7961(3)	281.2126(1)	288.2932(2)	253.7347(1)	260.1987(4)
M_{bb} / uÅ^2	51.5412(1)	51.5672(3)	50.1594(1)	50.3963(2)	53.8688(1)	54.4056(4)
M_{cc} / uÅ^2	3.2528(1)	3.2411(3)	40.1851(1)	40.4421(2)	46.4810(1)	46.4913(4)
κ	-0.971	-0.972	-0.977	-0.978	-0.976	-0.976

[a] A, B, and C are the rotational constants. D_J, D_{JK}, D_K, d_1, and d_2 are the quartic centrifugal distortion constants in the S-reduced semirigid rotor Hamiltonian. χ_{aa}, χ_{bb}, and χ_{cc} are the nuclear quadrupole coupling constants in the principal inertial axis system representation. N is the number of quadrupole hyperfine components fitted. σ is the rms deviation of the fit. μ_a, μ_b, μ_c are the electric dipole moment components, yes (Y) or no(N) indicates if the corresponding transitions were observed. M_{gg} (g = a, b or c) are the planar moments of inertia, i.e. M_{cc} = $(I_{aa}+I_{bb}-I_{cc})/2$. κ =$(2B-A-C)/(A-C)$ is Ray's asymmetry parameter. [b] Standard errors in parentheses in units of the last digit. [c] Values in

the brackets are fixed to the values of the ^{35}Cl species. [d] Values marked with asterisk are fixed to the scaled ^{35}Cl parent species values.

Table 3. Experimental substitution coordinates (r_s) and theoretical equilibrium coordinates (r_e) (B3LYP-D3(BJ)/Def2-TZVP, MP2/aug-cc-pVTZ) of the Cl atom in the principal axes system of the ^{35}Cl species of 3ClPA.

AAZ-I	r_s	r_e B3LYP	r_e MP2
a (Å)	±2.4544(6)[a]	-2.4682	-2.4494
b (Å)	±0.09(2)	-0.1368	-0.1364
c (Å)	0 [b]	0 [b]	0 [b]
G'AZ-II	r_s	r_e-B3LYP	r_e-MP2
a (Å)	±1.8982(8)	-1.9162	-1.8607
b (Å)	±0.348(4)	-0.3787	-0.4128
c (Å)	±0.372(4)	-0.3474	-0.3265
GGZ-III	r_s	r_e-B3LYP	r_e-MP2
a (Å)	±1.813(1)	1.8448	1.7903
b (Å)	±0.531(3)	-0.5255	-0.5278
c (Å)	±0.08(2)	-0.0785	-0.1199

[a] Standard error in parentheses in units of the last digit using Costain's estimation. [b] Fixed to zero by symmetry.

Table 4. Experimental and theoretical NQC constants in the principal axis of the coupling tensor, and rotation angles of principal inertia tensor axes to EFG axis (*z*), and theoretical angles between the principal inertia tensor axis (*a, b, c*) and the Cl-C bond.

3ClPA		Exp	B3LYP (BJ) /Def2-TZVP	MP2/aug-cc-pVTZ	MP2//DK
^{35}Cl-I	χ_{xx} / MHz	35.5(3)[a]	37.8	33.5	34.6
	χ_{yy} / MHz	36.03(1)	38.5	34	34.8
	χ_{zz} / MHz	-71.6(3)	-76.3	-67.5	-69.4
	η[b] / °	0.007(5)	0.01	0.01	0
	$\lvert\theta_{za}\rvert$[c] / °	23.7(2)	23.6	23.9	23.8
	$\lvert\theta_{zb}\rvert$ / °	66.3(2)	66.4	66.1	66.2
	$\lvert\theta_{zc}\rvert$ / °	90.0(0)	90	90	90
	$\lvert\theta_{a}\rvert$[d] / °		23.2	23.4	
	$\lvert\theta_{b}\rvert$ / °		66.8	66.6	
	$\lvert\theta_{c}\rvert$ / °		90	90	
^{35}Cl-II	χ_{xx} / MHz	33.2(8)	37.1	32.7	33.9
	χ_{yy} / MHz	38.2(7)	39.3	34.8	35.9
	χ_{zz} / MHz	-71.3(8)	-76.4	-68.1	-69.8
	η[b] / °	0.07(2)	0.03	0.03	0.03
	$\lvert\theta_{za}\rvert$[c] / °	60.2(2)	59.2	61.4	61.3
	$\lvert\theta_{zb}\rvert$ / °	53.6(2)	51.5	47	47
	$\lvert\theta_{zc}\rvert$ / °	50.8(2)	53.7	56.4	56.5
	$\lvert\theta_{a}\rvert$[d] / °		121.2	119.1	
	$\lvert\theta_{b}\rvert$ / °		51.2	46.7	
	$\lvert\theta_{c}\rvert$ / °		54.4	56.4	
^{35}Cl-III	χ_{xx} / MHz	34.9(6)	37.4	33	34.5
	χ_{yy} / MHz	37.0(7)	38.9	34.4	35.4
	χ_{zz} / MHz	-71.9(1)	-76.3	-67.4	-69.9
	η[b] / °	0.03(1)	0.02	0.02	0.01
	$\lvert\theta_{za}\rvert$[c] / °	62.59(5)	61.3	63.2	63.1
	$\lvert\theta_{zb}\rvert$ / °	27.84(9)	29	28	116.9
	$\lvert\theta_{zc}\rvert$ / °	85.5(2)	86.1	82.6	82.6
	$\lvert\theta_{a}\rvert$[d] / °		119	117.3	
	$\lvert\theta_{b}\rvert$ / °		29.4	28.5	
	$\lvert\theta_{c}\rvert$ / °		85.8	82.3	

[a] Standard error in parentheses in units of the last digit. [b] $\eta=(\chi_{xx}-\chi_{yy})/\chi_{zz}$. [c] Angles between the electric field gradient *z*-axis and the principal inertial axes (*a, b, c*). [d] Angles between the C-Cl bond axis and the principal inertial axes (*a, b, c*).

.

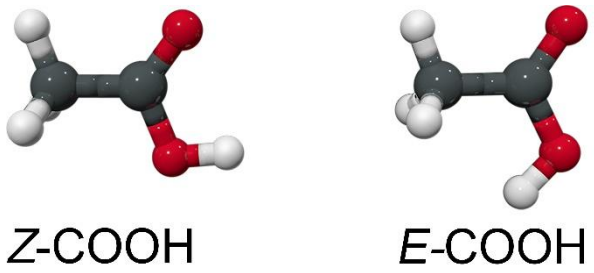

Figure 1. *Z*-COOH (carboxylic hydrogen atom and the C=O bond in *cis* configuration) and *E*-COOH (carboxylic hydrogen atom and the C=O bond in *trans* configuration) forms of acetic acid, the prototype carboxylic acid structure.

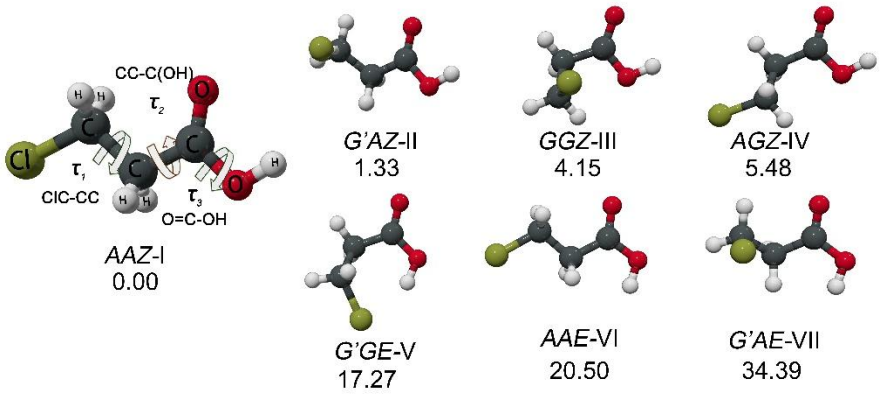

Figure 2. Structures and zero point corrected relative energies (ΔE_0) (kJ mol^{-1}) of the seven conformers of 3ClPA (B3LYP-D3(BJ)/Def2-TZVP).

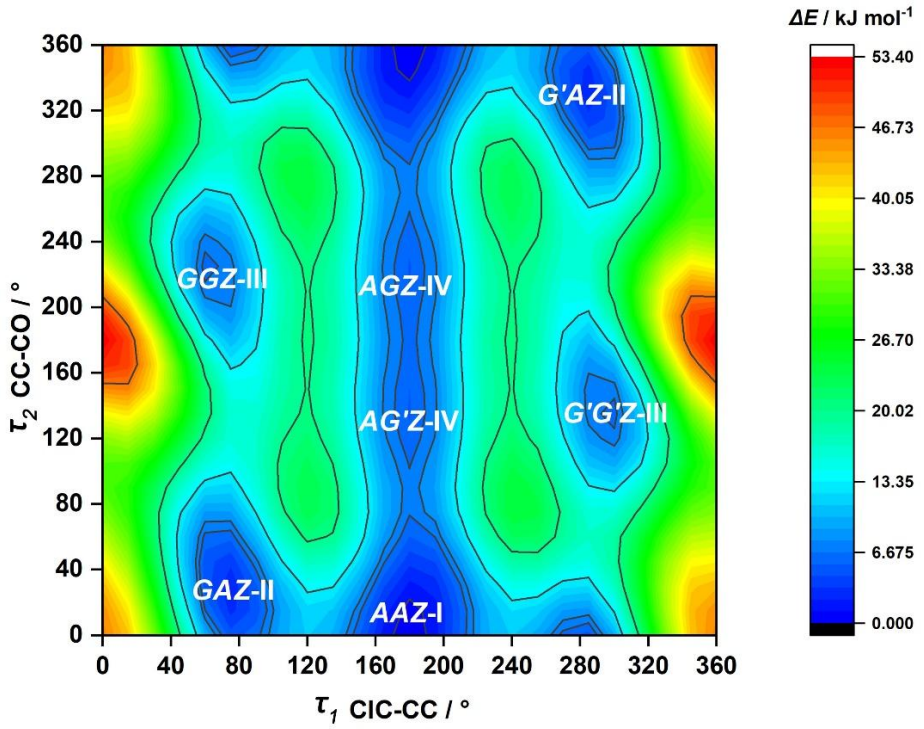

Figure 3. 2D potential energy diagram (reported values in kJ mol^{-1}) of 3ClPA with respect to τ_1 and τ_2. Relaxed scans of the dihedral angles were performed at the B3LYP-D3(BJ)/Def2-TZVP level of calculation using a 10° step in the full cycle of rotation.

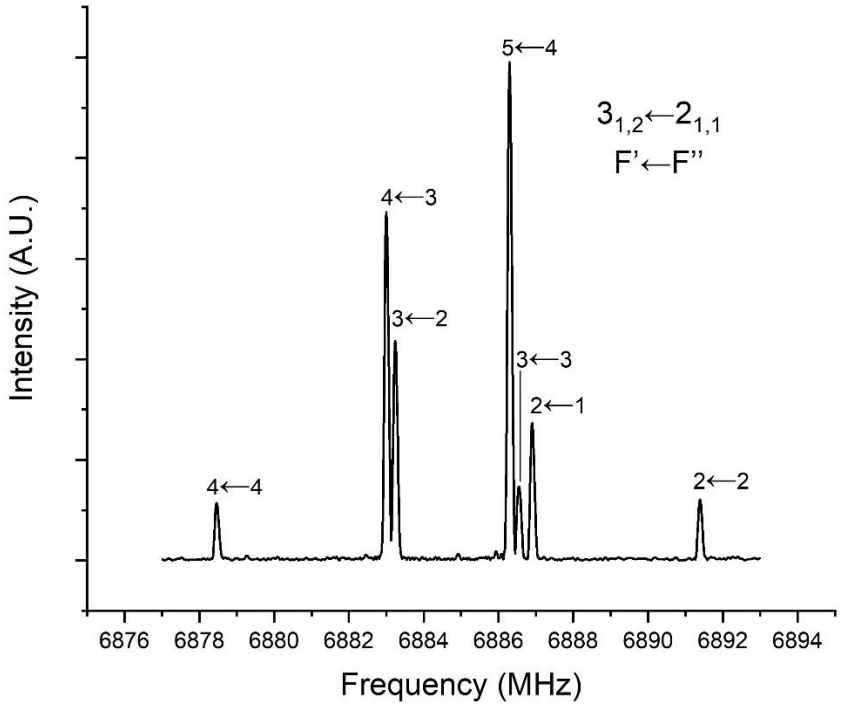

Figure 4. Details of the quadrupole hyperfine structure of the 31,2←21,1 transition of 35Cl-I. Hyperfine components are labelled as F' ←F'' where F = I + J and half integer spins are rounded up to the next integer.

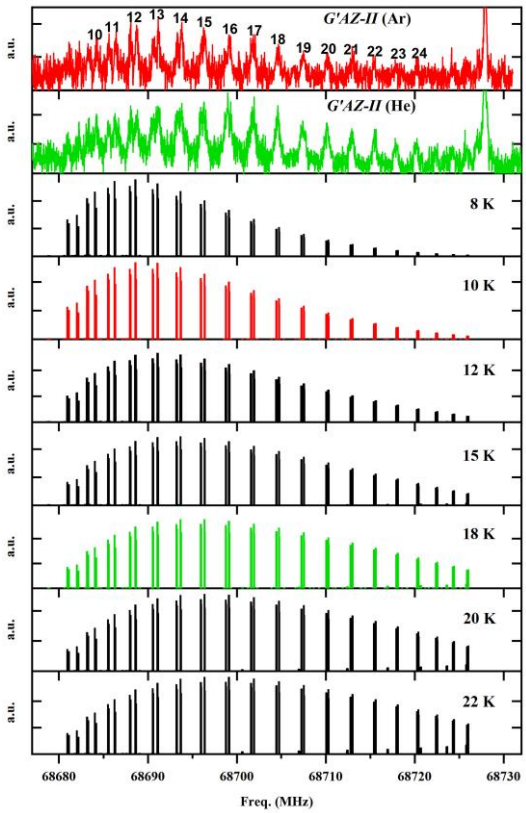

Figure 5. The K_a=9←8 Q-branch transitions of *G'AZ*-II can be recognized in the spectra recorded using Ar (upper red trace) and He (lower green trace). Numbers above the peaks indicate the assigned rotational quantum numbers (*J*). Simulated spectra of *G'AZ*-II at *T*= 8, 10, 12, 20 and 22 K using the SPCAT program considering the dipole moment component values (B3LYP-D3(BJ)/Def2-TZVP). On the right-hand side of the recorded spectrum is a μ_b-R-type transition line with *J*=13←12 and K_a=3←2 at 68727.85 MHz assigned to *AAZ*-I.

References

(1) Montes, R.; Rodil, R.; Cela, R.; Quintana, J. B. Determination of Persistent and Mobile Organic Contaminants (PMOCs) in Water by Mixed-Mode Liquid Chromatography-Tandem Mass Spectrometry. *Anal. Chem.* **2019**, *91* (8), 5176-5183. DOI: 10.1021/acs.analchem.8b05792.

(2) Schulze, S.; Zahn, D.; Montes, R.; Rodil, R.; Quintana, J. B.; Knepper, T. P.; Reemtsma, T.; Berger, U. Occurrence of emerging persistent and mobile organic contaminants in European water samples. *Water Res.* **2019**, *153*, 80-90. DOI: 10.1016/j.watres.2019.01.008.

(3) Reemtsma, T.; Berger, U.; Arp, H. P.; Gallard, H.; Knepper, T. P.; Neumann, M.; Quintana, J. B.; Voogt, P. Mind the Gap: Persistent and Mobile Organic Compounds-Water Contaminants That Slip Through. *Environ. Sci. Technol.* **2016**, *50* (19), 10308-10315. DOI: 10.1021/acs.est.6b03338.

(4) Arp, H. P.; Niederer, C.; Goss, K. U. Predicting the partitioning behavior of various highly fluorinated compounds. *Environ. Sci. Technol.* **2006**, *40* (23), 7298-7304. DOI: 10.1021/es060744y.

(5) Kumar, S.; Singh, S. K.; Calabrese, C.; Maris, A.; Melandri, S.; Das, A. Structure of saligenin: microwave, UV and IR spectroscopy studies in a supersonic jet combined with quantum chemistry calculations. *Phys. Chem. Chem. Phys.* **2014**, *16* (32), 17163-17171. DOI: 10.1039/c4cp01693a.

(6) Melandri, S.; Evangelisti, L.; Maris, A.; Caminati, W.; Giuliano, B. M.; Feyer, V.; Prince, K. C.; Coreno, M. Rotational and core level spectroscopies as complementary techniques in tautomeric/conformational studies: the case of 2-mercaptopyridine. *J. Am. Chem. Soc.* **2010**, *132*

(30), 10269-10271. DOI: 10.1021/ja104484b.

(7) Xie, F.; Tikhonov, D. S.; Schnell, M. Electric nuclear quadrupole coupling reveals dissociation of HCl with a few water molecules. *Science* **2024**, *384* (6703), 1435-1440. DOI: 10.1126/science.ado7049.

(8) Andrews, J. E.; Nichols, H. P.; Schmid, J. E.; Mole, L. M.; Hunter, E. S., 3rd; Klinefelter, G. R. Developmental toxicity of mixtures: the water disinfection by-products dichloro-, dibromo- and bromochloro acetic acid in rat embryo culture. *Reprod. Toxicol.* **2004**, *19* (1), 111-116. DOI: 10.1016/j.reprotox.2004.06.005.

(9) Mesri, S.; Wahab, R. A.; Huyop, F. Degradation of 3-chloropropionic acid (3CP) byPseudomonas sp. B6P isolated from a rice paddy field. *Ann. Microbiol.* **2009**, *59* (3), 447-451. DOI: 10.1007/BF03175129.

(10) Hamid, A. A. A.; Wong, E. L.; Joyce-Tan, K. H.; Shamsir, M. S.; Hamid, T. H. T. A.; Huyop, F. Molecular Modelling and Functional Studies of the Non-Stereospecific *α*-Haloalkanoic Acid Dehalogenase (DehE) fromRhizobiumSP. RC1 and its Association with 3-Chloropropionic Acid (β-Chlorinated Aliphatic Acid). *Biotechnol. Biotec. Eq.* **2014**, *27* (2), 3725-3736. DOI: 10.5504/bbeq.2012.0142.

(11) Yang, M.; Zhang, X.; Liang, Q.; Yang, B. Application of (LC/)MS/MS precursor ion scan for evaluating the occurrence, formation and control of polar halogenated DBPs in disinfected waters: A review. *Water Res.* **2019**, *158*, 322-337. DOI: 10.1016/j.watres.2019.04.033.

(12) Muslem, W. H.; Edbeib, M. F.; Aksoy, H. M.; Kaya, Y.; Hamid, A. A. A.; Hood, M. H. M.; Wahab, R. A.; Huyop, F. Biodegradation of 3-chloropropionic acid (3-CP) by Bacillus cereus WH2 and its in silico enzyme-substrate docking analysis. *J. Biomol. Struct. Dyn.* **2020**, *38* (11), 3432-3441. DOI: 10.1080/07391102.2019.1655482.

(13) Gallidabino, M. D.; Hamdan, L.; Murphy, B.; Barron, L. P. Suspect screening of halogenated carboxylic acids in drinking water using ion exchange chromatography - high resolution (Orbitrap) mass spectrometry (IC-HRMS). *Talanta* **2018**, *178*, 57-68. DOI: 10.1016/j.talanta.2017.08.092.

(14) Hadi, A., Greene, A. Isolation and identification of 3-chloropropionic acid degrading bacterium from Oxley Creek, Queensland, Australia. In *AIP Conference Proceedings*. **2019**, 2155, 1. DOI: 10.1063/1.5125536

(15) Calabrese, C., Maris, A., Uriarte, I., Cocinero, E. J., Melandri, S. Effects of Chlorination on the Tautomeric Equilibrium of 2-Hydroxypyridine: Experiment and Theory. *Chem. Eur. J.*, **2017**, *23*(15), 3595-3604. DOI: 10.1002/chem.201604891.

(16) Lv, D.; Maris, A.; Evangelisti, L.; Maggio, A.; Song, W.; Elliott, A. A.; Peebles, S. A.; Neill, J. L.; Muckle, M. T.; Pate, B. H.; et al. σ-Hole activation and structural changes upon perfluorination of aryl halides: direct evidence from gas phase rotational spectroscopy. *Phys. Chem. Chem. Phys.* **2021**, *23* (33), 18093-18101. DOI: 10.1039/d1cp03023j.

(17) Evangelisti, L., Brendel, K., Mäder, H., Caminati, W., Melandri, S. Rotational spectroscopy probes water flipping by full fluorination of benzene. *Angew. Chem.*, **2017**, *129*(44), 13887-13891. DOI: 10.1002/ange.201707155.

(18) Hocking, W. H. The Other Rotamer of Formic Acid, cis-HCOOH[1]. *Z. Naturforsh. A*. **1976**, *31* (9), 1113-1121. DOI: 10.1515/zna-1976-0919.

(19) Senent, M. L. *Ab initio* determination of the torsional spectra of acetic acid. *Mol. Phys.* **2001**, *99* (15), 1311-1321. DOI: 10.1080/00268970110048374.

(20) Stiefvater, O. L. Microwave spectrum of propionic acid. I. Spectrum, dipole moment, barrier to internal rotation, and low-frequency vibrations of *cis*-propionic acid. *J. Chem. Phys.* **1975**, *62* (1), 233-243. DOI: 10.1063/1.430268.

(21) Stiefvater, O. L. Microwave spectrum of propionic acid. II. Structure of *cis*-propionic acid by double resonance modulation microwave spectroscopy. *J. Chem. Phys.* **1975**, *62* (1), 244-256. DOI: 10.1063/1.430269.

(22) Ilyushin, V. V.; Margulès, L.; Tercero, B.; Motiyenko, R. A.; Dorovskaya, O.; Alekseev, E. A.; Alonso, E. R.; Kolesniková, L.; Cernicharo, J.; Guillemin, J. C. Submillimeter wave spectroscopy of propanoic acid (CHCHCOOH) and its ISM search. *J. Mol. Spectrosc.* **2021**, *379*, 111454. DOI: ARTN 11145410.1016/j.jms.2021.111454.

(23) Jaman, A. I.; Chakraborty, S.; Chakraborty, R. Millimeterwave rotational spectrum and

theoretical calculations of propionic acid. *J. Mol. Spectrosc.* **2015**, *1079*, 402-406. DOI: 10.1016/j.molstruc.2014.09.004.

(24) Maçôas, E. M. S.; Khriachtchev, L.; Pettersson, M.; Fausto, R.; Räsänen, M. Internal rotation in propionic acid: Near-infrared-induced isomerization in solid Argon. *J. Phys. Chem. A.* **2005**, *109* (16), 3617-3625. DOI: 10.1021/jp044070u

(25) Van Eijck, B. P.; Van Der Plaats, G.; Van Roon, P. H. The molecular structure of monofluoroacetic acid. *J. Mol. Spectrosc.* **1972**, *11* (1), 67-91. DOI: 10.1016/0022-2860(72)85222-0.

(26) Van Eijck, B. P.; Dijkerman, H. A.; Smits, J. The microwave spectrum of bromoacetic acid. *J. Mol. Spectrosc.* **1978**, *73* (2), 305-310. DOI: 10.1016/0022-2852(78)90222-9.

(27) Van Eijck, B. P.; Maagdenberg, A. A. J.; Janssen, G.; van Goethem-Wiersma, T. J. The microwave spectrum of difluoroacetic acid. *J. Mol. Spectrosc.* **1983**, *98* (2), 282-303. DOI: 10.1016/0022-2852(83)90244-8.

(28) Stolwijk, V. M.; van Eijck, B. P. Microwave spectra and barriers to internal rotation of trifluoroacetic acid and trifluoroacetyl fluoride. *J. Mol. Spectrosc.* **1985**, *113* (1), 196-207. DOI: 10.1016/0022-2852(85)90130-4.

(29) Apóstolo, R. F. G.; Bazsó, G.; Bento, R. R. F.; Tarczay, G.; Fausto, R. The first experimental observation of the higher-energy trans conformer of trifluoroacetic acid. *J. Mol. Spectrosc.* **2016**,

1125, 288-295. DOI: 10.1016/j.molstruc.2016.06.077.

(30) Van Eijck, B. P.; Maagdenberg, A. A. J.; Wanrooy, J. The microwave spectrum of monochloroacetic acid. *J. Mol. Spectrosc.* **1974**, *22* (1), 61-67. DOI: 10.1016/0022-2860(74)80067-0.

(31) Fausto, R.; Teixeira-Dias, J. J. C.; Gil, F. P. S. C. Conformers, vibrational spectra and laser-induced rotamerization of $CH_2ClCOOH$. *J. Chem. Soc., Faraday Trans.* **1993**, *89* (17). DOI: 10.1039/ft9938903235.

(32) Van Zoeren, E.; Van Eijck, B. P. The microwave spectrum of α-fluoropropionic acid. *J. Mol. Spectrosc.* **1984**, *103* (1), 75-86. DOI: 10.1016/0022-2852(84)90147-4.

(33) Lesarri, A.; Grabow, J.-U.; Caminati, W. Conformation of chiral molecules: The rotational spectrum of 2-chloropropionic acid. *Chem. Phys. Lett.* **2009**, *468* (1-3), 18-22. DOI: 10.1016/j.cplett.2008.11.053.

(34) Melandri, S.; Caminati, W.; Favero, L. B.; Millemaggi, A.; Favero, P. G. A Microwave Free Jet Absorption Spectrometer and Its First Applications. *J. Mol. Spectrosc.* **1995**, *352*, 253-258. DOI: 10.1016/0022-2860(94)08516-K.

(35) Calabrese, C.; Vigorito, A.; Maris, A.; Mariotti, S.; Fathi, P.; Geppert, W. D.; Melandri, S. Millimeter Wave Spectrum of the Weakly Bound Complex CH_2=CHCN·H_2O: Structure, Dynamics, and Implications for Astronomical Search. *J. Phys. Chem. A*, **2015**, *119*(48), 11674-

11682. DOI: 10.1021/acs.jpca.5b08426.

(36) Song, W.; Maris, A.; Rivilla, V. M.; Fortuna, F.; Evangelisti, L.; Lv, D.; Rodríguez-Almeida, L.; Jiménez-Serra, I.; Martín-Pintado, J.; Melandri, S. Micro- and millimeter-wave spectra of five conformers of cysteamine and their interstellar search. *Astro. Astrophys.* **2022**, *661,* A129. DOI: 10.1051/0004-6361/202142958.

(37) Reiher, M. Relativistic Douglas–Kroll–Hess theory. *WIREs Comput. Mol. Sci.* **2011**, *2* (1), 139-149. DOI: 10.1002/wcms.67.

(38) Dunning, T. H. Gaussian basis sets for use in correlated molecular calculations. I. The atoms boron through neon and hydrogen. *J. Chem. Phys.* **1989**, *90* (2), 1007-1023. DOI: 10.1063/1.456153.

(39) Wilson, A. K.; Woon, D. E.; Peterson, K. A.; Dunning, T. H. Gaussian basis sets for use in correlated molecular calculations. IX. The atoms gallium through krypton. *J. Chem. Phys.* **1999**, *110* (16), 7667-7676. DOI: 10.1063/1.478678.

(40) Pritchard, B. P.; Altarawy, D.; Didier, B.; Gibson, T. D.; Windus, T. L. New Basis Set Exchange: An Open, Up-to-Date Resource for the Molecular Sciences Community. *J. Chem. Inf. Model.* **2019**, *59* (11), 4814-4820. DOI: 10.1021/acs.jcim.9b00725.

(41) Frisch M. J.; Trucks G. W.; Schlegel H. B.; Scuseria G. E.; Robb M. A.; Cheeseman J. R.; Scalmani G.; Barone V.; Petersson G. A.; Nakatsuji H.; Li X.; Caricato M.; Marenich A. V.; Bloino

J.; Janesko B. G.; Gomperts R.; Mennucci B.; Hratchian H. P.; Ortiz J. V.; Izmaylov A. F.; Sonnenberg J. L.; Williams-Young D.; Ding F.; Lipparini F.; Egidi F.; Goings J.; Peng B.; Petrone A.; Henderson T.; Ranasinghe D.; Zakrzewski V. G.; Gao J.; Rega N.; Zheng G.; Liang W.; Hada M.; Ehara M.; Toyota K.; Fukuda R.; Hasegawa J.; Ishida M.; Nakajima T.; Honda Y.; Kitao O.; Nakai H.; Vreven T.; Throssell K.; Montgomery J. A. Jr.; Peralta J. E.; Ogliaro F.; Bearpark M. J.; Heyd J. J.; Brothers E. N.; Kudin K. N.; Staroverov V. N.; Keith T. A.; Kobayashi R.; Normand J.; Raghavachari K.; Rendell A. P.; Burant J. C.; Iyengar S. S.; Tomasi J.; Cossi M.; Millam J. M.; Klene M.; Adamo C.; Cammi R.; Ochterski J. W.; Martin R. L.; Morokuma K.; Farkas O.; Foresman J. B.; Fox D. J.. *Gaussian 16*, Revision C.01; Gaussian, Inc.: Wallingford, CT, **2016**.

(42) Vigorito, A.; Calabrese, C.; Melandri, S.; Caracciolo, A.; Mariotti, S.; Giannetti, A.; Massardi, M.; Maris, A. Millimeter-wave spectroscopy and modeling of 1,2-butanediol. *Astron. Astrophys.* **2018**, *619*, A140. DOI: 10.1051/0004-6361/201833489.

(43) Pickett, H. M. The fitting and prediction of vibration-rotation spectra with spin interactions. *J. Mol. Spectrosc.* **1991**, *148* (2), 371-377. DOI: 10.1016/0022-2852(91)90393-o.

(44) Watson, J. K. Vibrational spectra and structure. Elsevier Amsterdam: **1977,** 1-89.

(45) Bragg, J. K. The Interaction of Nuclear Electric Quadrupole Moments with Molecular Rotation in Asymmetric-Top Molecules. I. *Phys. Rev.* **1948**, *74* (5), 533-538. DOI: 10.1103/PhysRev.74.533.

(46) Ruoff, R.; Klots, T.; Emilsson, T.; Gutowsky, H. Relaxation of conformers and isomers in

seeded supersonic jets of inert gases. *J. Chem. Phys.* **1990**, *93* (5), 3142-3150. DOI: 10.1063/1.458848.

(47) Vigorito, A.; Calabrese, C.; Paltanin, E.; Melandri, S.; Maris, A. Regarding the torsional flexibility of the dihydrolipoic acid's pharmacophore: 1,3-propanedithiol. *Phys. Chem. Chem. Phys.* **2016**, *19* (1), 496-502. DOI: 10.1039/c6cp05606g.

(48) Florio, G. M.; Christie, R. A.; Jordan, K. D.; Zwier, T. S. Conformational preferences of jet-cooled melatonin: probing trans- and *cis*-amide regions of the potential energy surface. *J. Am. Chem. Soc.* **2002**, *124* (34), 10236-10247. DOI: 10.1021/ja0265916.

(49) Godfrey, P. D.; Brown, R. D. Proportions of Species Observed in Jet Spectroscopy−Vibrational Energy Effects: Histamine Tautomers and Conformers. *J. Am. Chem. Soc.* **1998**, *120* (41), 10724-10732. DOI: 10.1021/ja980560m.

(50) Carlson, C. D.; Seifert, N. A.; Heger, M.; Xie, F.; Thomas, J.; Xu, Y. J. Conformational dynamics of 1-phenyl-2,2,2-trifluoroethanol by rotational spectroscopy and calculations. *J. Mol. Spectrosc.* **2018**, *351*, 62-67. DOI: 10.1016/j.jms.2018.07.006.

(51) PyykkÖ, P. Spectroscopic nuclear quadrupole moments. *Mol. Phys.* **2001**, *99* (19), 1617-1629. DOI: 10.1080/00268970110069010.

(52) Blanco, S.; Lesarri, A.; Lopez, J. C.; Alonso, J. L. The gas-phase structure of alanine. *J. Am. Chem. Soc.* **2004**, *126* (37), 11675-11683. DOI: 10.1021/ja048317c.

(53) Kraitchman. Determination of molecular structure from microwave spectroscopic data. *Am. J. Phys.* **1953**, *21* (1), 17-24. DOI: 10.1119/1.1933338.

(54) Costain, C. Further comments on the accuracy of *rs* substitution structures. *Trans. Am. Crystallogr. Assoc*, **1966**, *2*, 157-164.

(55) Baroncelli, F.; Panizzi, G.; Evangelisti, L.; Melandri, S.; Maris, A. Structure and nuclear quadrupole coupling interaction in hydroxylamines: The rotational spectrum of diethyl(H)hydroxylamine. *J. Mol. Spectrosc.* **2023**, *392*, 111759. DOI: 10.1016/j.jms.2023.111759.

(56) Kisiel, Z. Assignment and Analysis of Complex Rotational Spectra. In *Spectroscopy from Space*, Demaison, J., Sarka, K., Cohen, E. A. Eds.; Springer Netherlands, **2001**; pp 91-106.

(57) de Luis, A.; Sanz, M. E.; Lorenzo, F. J.; López, J. C.; Alonso, J. L. Internal Rotation and the Chlorine Nuclear Quadrupole Coupling Tensor of 1-Chloropropane. *J. Mol. Spectrosc.* **1997**, *184* (1), 60-77. DOI: 10.1006/jmsp.1997.7298.

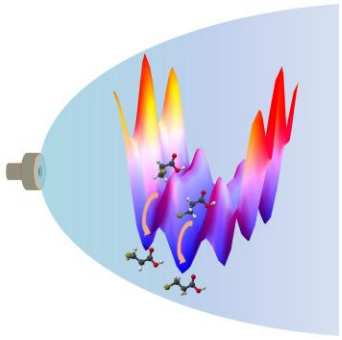

For Table of Contents Only